A Hybrid FDTD/Radiative Transfer Method for Modeling Remote Sensing Observations of Snow

Jon W. Wallace and Michael A. Jensen
Department of Electrical and Computer Engineering, Brigham Young University
459 Clyde Building Brigham Young University Provo, UT, 84602-4099
Tel: 801-378-5736 Fax: 801-378-6586 Email: wallacej@et.byu.edu, jensen@ee.byu.edu

INTRODUCTION

Trends in large snow and ice masses on the earth are an indicator of global environmental change. Thus, characterization of emission and scatter behavior of snow and ice continues to be an area of active research for the remote sensing community. Snow and ice tend to be complex media which are difficult to model analytically. Also, purely numerical techniques quickly exhaust available computational resources. We propose a hybrid FDTD/radiative transfer technique to overcome the limitations of purely numerical or analytical techniques.

FDTD/RADIATIVE TRANSFER METHOD

One efficient solution for obtaining scattering and emission behavior from large geophysical objects comes from radiative transfer theory [1], [2], [3]. Recent work [4] has employed advanced electromagnetic modeling with the Monte Carlo technique to obtain radiative transfer quantities (phase matrices and extinction coefficients) for densely packed spheres. This work has used T-matrix methods, which are difficult to apply to general media (non-spherical particles, for example). Our approach is to use FDTD [5], [6] to obtain the radiative transfer quantities, allowing characterization of arbitrary media.

In radiative transfer, phase matrices and extinction coefficients characterize scattering behavior of a random medium and are ensemble averages. The phase matrix is given by

$$\overline{\overline{P}} = \lim_{\Delta V \to \infty} \frac{1}{\Delta V} \mathbf{E}\left[\overline{\overline{L}}(\Delta V)\right] \tag{1}$$

where ΔV is the test volume size, $\overline{\overline{L}}$ is the Stokes matrix for a given volume size, and $\mathbf{E}[\cdot]$ represents an expectation. The scattering and absorption coefficients are given by

$$k_s = \lim_{\Delta V \to \infty} \frac{1}{\Delta V} \frac{\mathbf{E}[P_s(\Delta V)]}{S_i} \tag{2}$$

$$k_a = \lim_{\Delta V \to \infty} \frac{1}{\Delta V} \frac{\mathbf{E}[P_a(\Delta V)]}{S_i} \tag{3}$$

where P_s is total power scattered, P_a is total power absorbed, and S_i is incident power density.

In the Monte Carlo technique, these ensemble averages are approximated by averaging over many random realizations generated according to the proper statistical distribution. To calculate these quantities numerically, a finite test volume (ΔV) is required which exhibits two characteristics not present in the infinite volume. First, surface scattering results as waves cross the domain boundary. This effect can be removed by decomposing scattered fields into a coherent part (due to artificial boundary scattering) and an incoherent part (due to the random volume). This decomposition is given by

$$\overline{E}_s = \mathbf{E}\left[\overline{E}_s\right] + \overline{\mathcal{E}}_s \tag{4}$$

where $\overline{E}_s$ is scattered electric field. Thus, when approximating (1)-(3), incoherent fields ($\overline{\mathcal{E}}_s$) are used instead of total scattered fields. Second, a finite domain will introduce artificial correlation of scatterers at the domain boundary. This effect is removed by making the test volume large.

Our work suggests the use of a simple convergence study as a method for determining the test volume size and the number of random realizations required to mitigate finite volume effects.

CONVERGENCE STUDY

In order to apply the FDTD/radiative transfer method, a knowledge of the minimum test volume size and random realizations is required. Otherwise, simulation results will be difficult to interpret and apply. We compared the phase matrices for Mie spheres for (1) the exact analytical solution for an infinite volume of independently scattering spheres, and (2) the approximate Monte Carlo solution for a finite volume of spheres. Figs. 1 and 2 show average fractional error and average absolute fractional error between the two cases as a function of volume size and number of random realizations. These two metrics are given by

$$\text{Average Error} = \frac{1}{N}\sum_{n=1}^{N} \frac{P_{n,\text{th}} - P_n}{P_{n,\text{th}}}$$

$$\text{Absolute Error} = \frac{1}{N}\sum_{n=1}^{N} \left|\frac{P_{n,\text{th}} - P_n}{P_{n,\text{th}}}\right|. \tag{5}$$

0-7803-6359-0/00/$10.00 © 2000 IEEE

where $P_{n,\text{th}}$ is the exact theoretical phase matrix quantity and P_n is the simulated quantity at angle number n.

A cubical test volume size of 5λ per side with 32 realizations was deemed a good tradeoff between simulation accuracy and required computational time.

FDTD PHASE MATRICES

Fig. 3 shows the cubical test volume used in the FDTD simulations. First, to test validity of the method, a sparse distribution of particles (2% fractional volume) was modeled and compared to the analytical solution for independent Mie scattering. The phase matrix quantities P_{11} and P_{22} are plotted in Fig. 4.

The Monte Carlo solution applied in the convergence study for 256 realizations is very close to the analytical solution. The FDTD solution for 32 realizations oscillates about the correct solution, which is consistent with our convergence study and shows the hybrid technique is valid.

Next, we turn to a more dense medium (20% fractional volume), which would be more representative of real snow in Fig. 5. In this case, we compare the results to QCA-CP [2], an accepted theory for densely packed spheres. As expected, the independent Mie solution predicts scatter which is too high. The Monte Carlo Mie solution assumes only single scattering of fields, and predicts scatter which is too low. The FDTD solution compares favorably with the QCA-CP scaled solution. However, apparent in P_{22} is an upward trend in FDTD as opposed to a downward trend in the QCA-CP scaled solution. This result suggests that the density of a medium affects not only the level of scattering, but also (to a lesser degree) the shape of the phase matrix curves.

Finally, to show the power of FDTD for modeling arbitrary media, we applied the method to penetrating spheres. Spheres are placed according to a uniform distribution as before except that they are allowed to overlap. Enough cells are filled to meet the volume fill fraction requirement, with a given cell being counted only once even if it is contained in two or more spheres.

Fig. 6 compares the plot of P_{11} resulting from this simulation with curves from all of the methods considered in this paper applied to non-penetrating spheres. These results indicate a 5 fold increase in P_{11} when a penetrating model is used, with the value for the penetrating particles being even larger than that from the independent scattering solution. Research in [4] has modeled similar dense media using "sticky particles," which also exhibited a dramatic increase in scattering levels.

REFERENCES

[1] S. Chandrasekhar, Radiative Transfer, Oxford: Clarendon Press, 1950.

[2] L. Tsang, J. A. Kong, R. T. Shin, Theory of Microwave Remote Sensing, 119-207, 498-505, 1985.

[3] L. Tsang, A. Ishimaru, "Radiative wave equations for vector electromagnetic propagation in dense nontenuous media," Journal of Electromagnetic Waves and Applications, vol. 1, no. 1, pp. 59-72, 1987.

[4] L. M. Zurk, L. Tsang, D. P. Winebrenner, "Scattering properties of dense media from Monte Carlo simulations with application to active remote sensing of snow," Radio Science, vol. 31, no. 4, pp. 803-819, 1996.

[5] K. S. Yee "Numerical solution of initial boundary value problem involving Maxwell's equations in isotropic media," IEEE Transactions on Antennas and Propagation, AP-14, pp. 302-307, 1966.

[6] A. Taflove, Computational Electrodynamics: The Finite Difference Time Domain Method, Boston: Artech House, 1995.

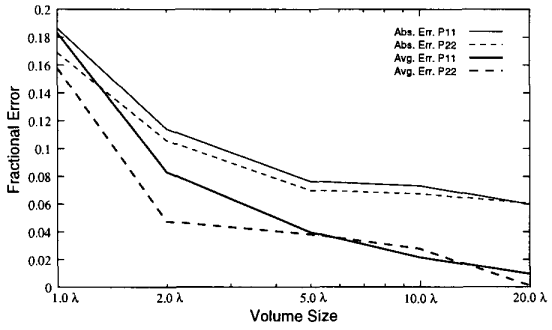

Figure 1: Plot of average and absolute error for P_{11} and P_{22} as a function of the test volume cube length. Simulation parameters were scatterer radii $a = 0.1\lambda$, fractional volume $f = 10\%$, realizations $N = 256$, and scatterer dielectric constant $\epsilon_s = 3.2\epsilon_0$.

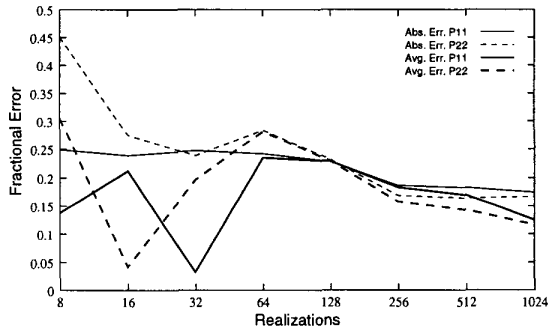

Figure 2: Plot of average and absolute error for P_{11} and P_{22} as a function of the number of realizations (N). Simulation parameters were scatterer radii $a = 0.1\lambda$, fractional volume $f = 10\%$, test volume cube length 1λ, and scatterer dielectric constant $\epsilon_s = 3.2\epsilon_0$.

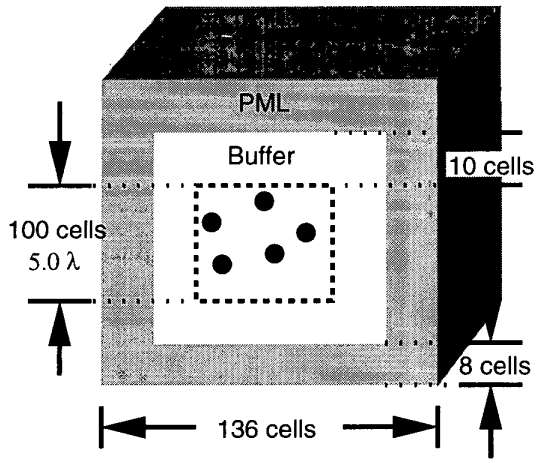

Figure 3: Simulation test volume cube for FDTD simulations

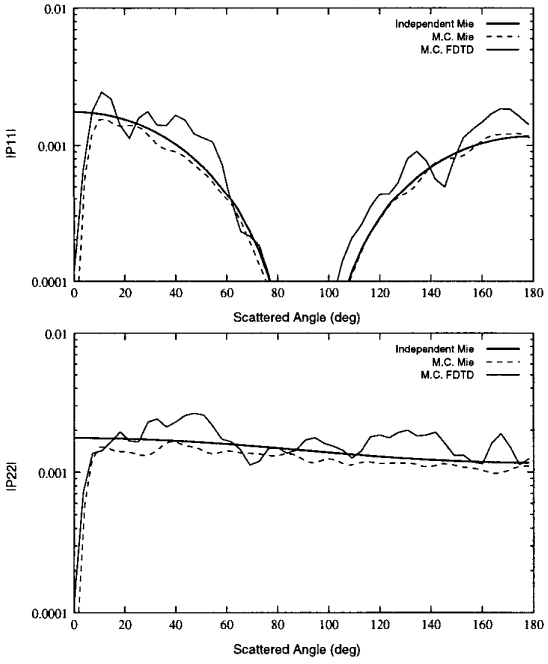

Figure 4: Phase matrix components given by FDTD simulations for a sparse distribution of non-penetrating spheres. Parameters were $a = 0.1\lambda$, cube length 5λ, $N = 32$, $f = 2\%$, and $\epsilon_s = 3.2\epsilon_0$.

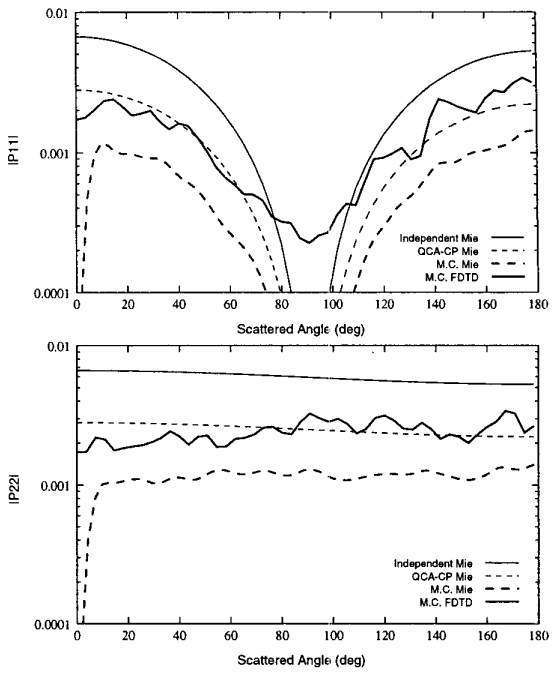

Figure 5: Phase matrix components given by FDTD simulations for a dense distribution of non-penetrating spheres. Parameters were $a = 0.075\lambda$, cube length 5λ, $N = 32$, $f = 20\%$, and $\epsilon_s = 3.2\epsilon_0$.

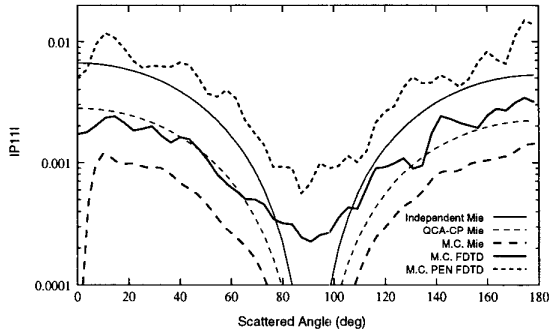

Figure 6: Phase matrix component given by FDTD simulations for a dense distribution of penetrating spheres. Parameters were $a = 0.075\lambda$, cube length 5λ, $N = 32$, $f = 20\%$, and $\epsilon_s = 3.2\epsilon_0$.